High Traction Differentials

Dr. Hermann J. Stadtfeld

How a ratio change can improve traction. The schematic graphic (Fig. 1) shows an unrolled differential with the planetary pinion in the center and the side gears left and right. Forward driving is accomplished in this model by moving all three gears from their top position in Figure 1 to the middle position and down to the lower position. In case of good traction, this is happening without any relative rotation of the three shown differential gears. In case the left wheel (which is connected to the left-side gear) slips, then in the model the left-side gear will rotate clockwise, while the unit moves downwards in the graphic. This will cause a counterclockwise rotation of the planetary pinion while it rotates together with the differential carrier around the axis of the two side gears.

In the model this means the right-side gear rotates clockwise with the same speed as the carrier does. The carrier rotation adds to the left-side gear rotation, which makes the left wheel of the vehicle spin with twice the rpm of the carrier. On the right side, the carrier speed offsets the right-side gear speed, such that the right wheel is not rotating at all. The vehicle is stuck, with no torque on the right-side wheel and no traction on the left-side wheel.

In the high-traction differential, the ratio between the planetary pinion and the side gears changes as a rotation like described happens. The rotation shown in the graphic from bottom to top moves the line of action from a small radius R_2^* in the right-side gear and a large radius R_1^* in the planetary pinion, to an increasing radius of the right-side gear and a decreasing radius of the planetary pinion. At the middle graphic, the line of action crosses the pitch line at the center distance line, which splits the center distance exactly in the two pitch radii. This means the ratio is equal to the division of the number of teeth of the sun gear and the planetary pinion (also: ratio $= R_2/R_1$). The ratio in the bottom graphic is smaller and the ratio in the top graphic is larger due to the line of action shift. The engagement between the planetary pinion and the left-side gear behaves in the opposite way, which squares the ratio increase factor from bottom to top.

In the case of a differential with involute teeth (constant ratio), the contact force, which was reduced by the free spinning left wheel, will first reduce and then eliminate the traction of the right wheel. The high-traction design will, in the case of a left-wheel traction loss, instantly increase the ratio, which accelerates the left wheel. The acceleration causes a reaction torque in forward driving direction on the non-rotating right wheel. In other words, at the instant the planetary pinion reduces the contact force to the right-side gear, the ratio change will compensate this due to the increase of the lever arm R_2^{**} and "inject" a torque spike to the right wheel.

Of course, after one tooth mesh the sequence starts at the bottom of the graphic again. So what happens now? Nothing to worry about, in the contrary! At first, the ratio becomes low, which reduces the speed of the left wheel, such that the acceleration cycle can begin again, and the next torque spike to the right wheel in driving direction, can be generated. As long as the spinning wheel has some friction contact, the speed reduction of the spinning wheel by the ratio change will only prepare the differential for the generation of the next torque spike to the wheel with traction. The kinetic energy, stored the rotating differential carrier and the spinning wheel will remain nearly constant, while part of this energy is shifted between the spinning wheel and the differential carrier — without influencing transmission or engine of the vehicle.

One complete cycle of the sequence (Fig. 1) only lasts a fraction of a second, which is why the unit constantly provides torque impulses to the wheel which has traction, while the other wheel spins free.

The high-traction differential works like a reverse ABS. It gives active torque impulses, not just passive break application, like most electronic traction control systems.

The solution. A ratio factor $f_{R\text{-}Top} = x / y$ is defined. This is the maximal change of the ratio from the pitch circle to the top of the sun gear. A second ratio factor $f_{R\text{-}Root}$ represents the maximal
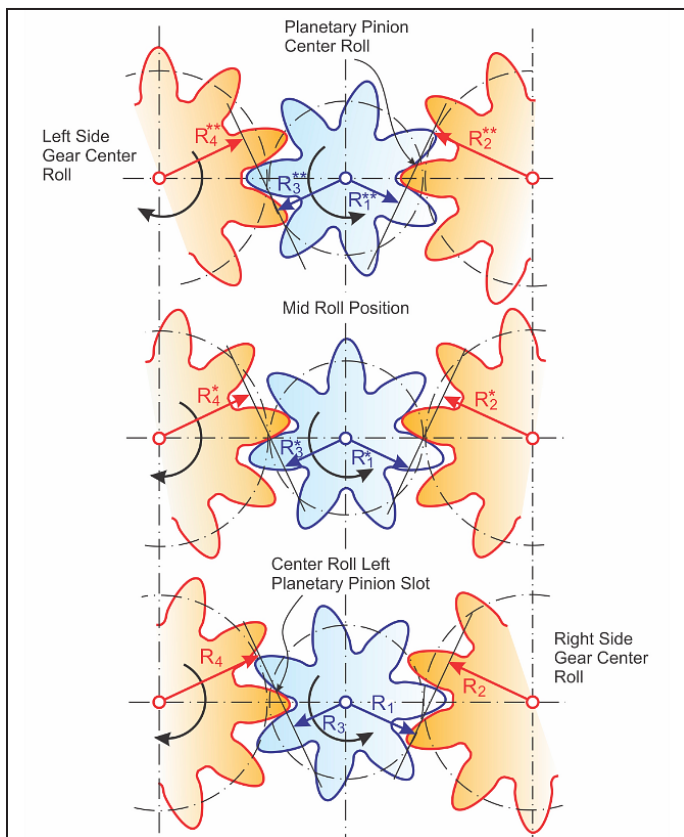

Figure 1   Principle of ratio change, from bottom to top.

change from the pitch line of the sun gear to its root. $f_{R\text{-}Root}$ is $1/f_{R\text{-}Top}$.

Y_{Top} is the factor; the effective gear radius has to change from pitch to top →
$$R_{eff\text{-}Top} = R_{Pitch} * Y_{Top}.$$
Y_{Root} is the factor; the effective gear radius has to change from pitch to root →
$$R_{eff\text{-}Root} = R_{Pitch} * Y_{Root}$$
X_{Top} is the factor; the effective pinion radius has to change from pitch to top →
$$R_{eff\text{-}Top} = R_{Pitch} * X_{Top}$$
X_{Root} is the factor; the effective pinion radius has to change from pitch to root→
$$R_{eff\text{-}Root} = R_{Pitch} * X_{Root}$$

Figure 2 Coast side ratio change along roll positions.

In the manufacturing straight bevel gear generator, the cutter cone distance is basically equal to the mean cone distance, which is R_M. If the effective radius of the gear has to change, while R_M remains constant, then this can be accomplished with a ratio of roll change.

It is at the center of roll:
$$RA = R_M/R_{Work} \qquad (1)$$

delivers in the center of roll position the predetermined $RA = RA0$

It should be realized at the gear top:
$$RA_{Gear\text{-}Top} = R_M/(R_{Work} * Y_{Top}) = RA0 / Y_{Top} \qquad (2)$$

It should be realized at the gear root:
$$RA_{Gear\text{-}Root} = R_M/(R_{Work} * Y_{Root}) = RA0 / Y_{Root} \qquad (3)$$

This provides sufficient information to construct the graph (Fig. 2); RA versus Δq or ΔW. Because of the difference between center of roll to top roll, and center of roll to bottom roll the graph (Fig. 2) is nonlinear. From its characteristic, a third order function is chosen in order to adequately approximate the graph.
$$RA = a + b\Delta W + cD \cdot W^2 + d\Delta W^3 \qquad (4)$$

The following boundary conditions are utilized to define the four coefficients in the RA equation:
$$\Delta W = 0 => a = RA = RA0 \qquad (5)$$

horizontal tangent at center of roll:
$$RA' = 0 \text{ at} \cdot W = 0 => RA' = b + 2c\Delta W + 3d\Delta W^2 => b = 0 \qquad (6)$$

at the root roll position:
$\Delta W = \Delta WE$ ... delta root roll angle
at the top roll position:
$\Delta W = \Delta WA$ ... delta top roll angle

Formulae (1) through (6) deliver the required coefficients. Now a coefficient comparison between formula (Ref. 4) and the Gleason modified roll formula will compute the machine basic setting modified roll coefficients.

Since Coniflex uses different basic settings and a sign change in the roll positions between the two flanks of one slot, the coefficients are calculated independently for the upper and lower Coniflex cutting.

In the pinion, the RA values have to be calculated separately using the X factor and the pinion $RA0$.

The application of the high-traction principle. The ratio factor f_R can be defined to realize the desired ratio change. In the Rockwell paper "High Traction Differential" from 1969 a theoretical value of 24% ratio change was used for the explanation.
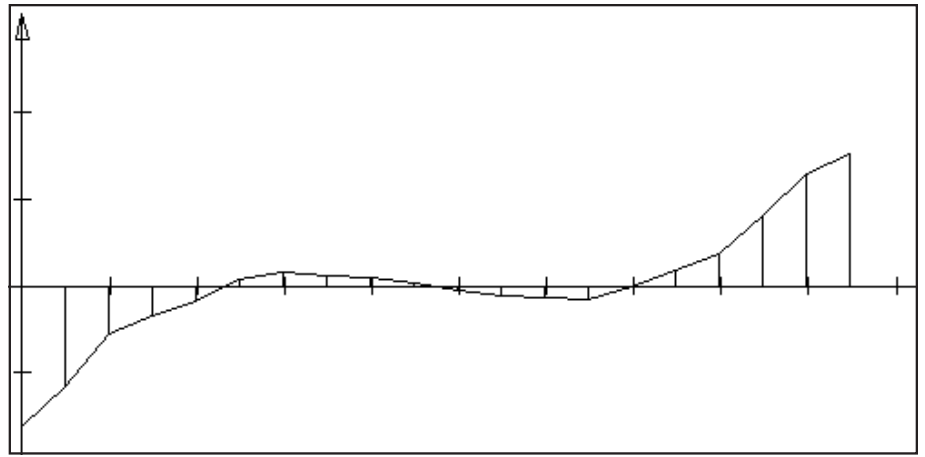
Developments in 1970 have shown that such a large change causes pointed topland on the gear member and severe undercut on the pinion member.

The developments, tests and optimizations during the years of high-traction applications, a standard of 15% ratio change between top and bottom roll position was found best-suitable, not only regarding tooth form but also regarding the function of the differential. Higher values showed unacceptably high tooth mesh impact, which eventually could cause unit failure due to tooth fracture.
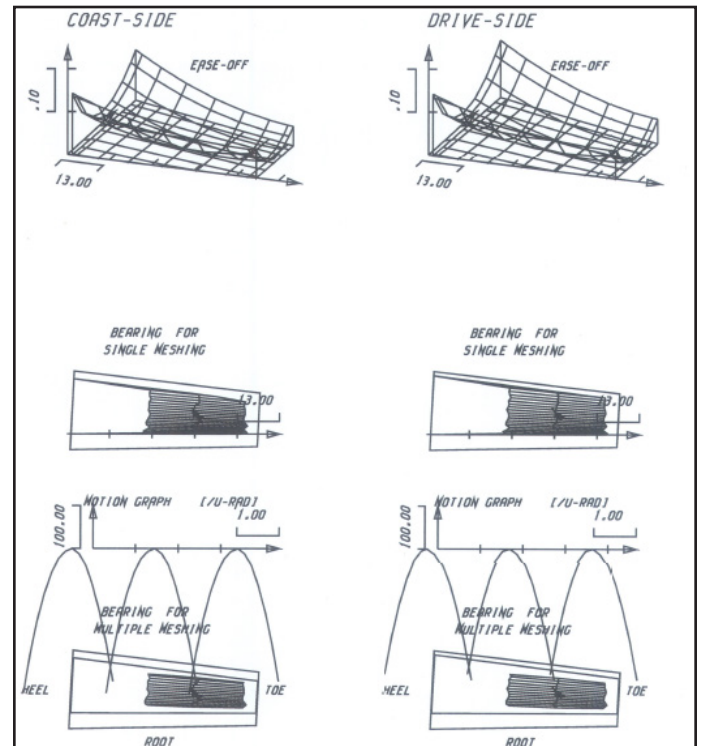

Figure 3 Ease-Off and TCA of regular straight bevel gear design.

Standard top ratio factor: $FR_{tp} = 0.93$
Standard root ratio factor: $FR_{rt} = 1 / FR_{tp} = 1.0753$
Overall ratio fluctuation factor: $FR_{Total} = 1.15 => 15\%$

The TCA of a Coniflex example as baseline is shown (Fig. 3). The simulation result of the ratio change between pinion and
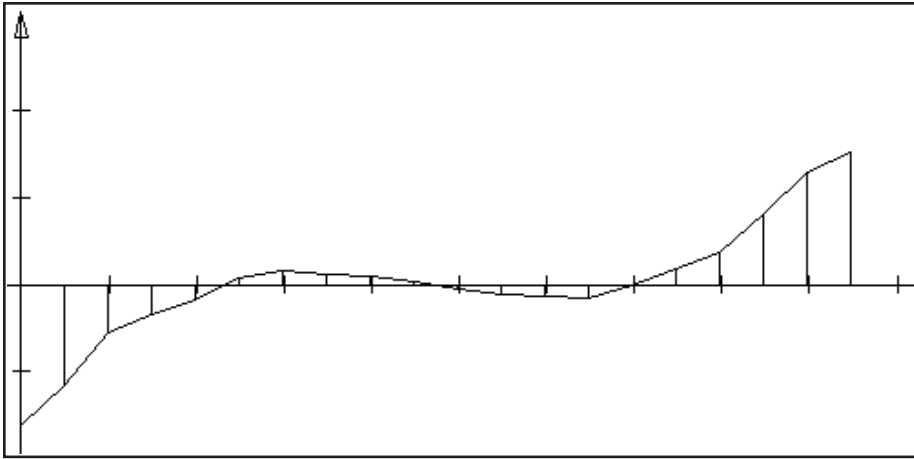
Figure 4   Coast (top) and drive side (bottom) ratio change along roll positions.

gear is plotted (Fig. 4). The 2 ratio graphs resemble exactly the desired characteristic.

A TCA of the same Coniflex gearset but now with high-traction profile by means of fourth-order modified roll is shown (Fig. 5). The Ease-Off topography shows a fourth-order function in profile. This is the world's first analytic tooth contact analysis ever made from a high-traction tooth profile. The Ease-Off shows a "Wildhaber-Novikov"-style shape. However, in case of Wildhaber-Novikov gearing, the modification of both interacting profiles will cancel in the interaction and result in constant transmission ratio. Here, two opposite modification curves result in an Ease-Off that shows the interaction between the two modified profiles as a W-shape.

The W-shaped Ease-Off is exactly as it was expected. The motion errors in Figures 3 and 4 also show that the modified
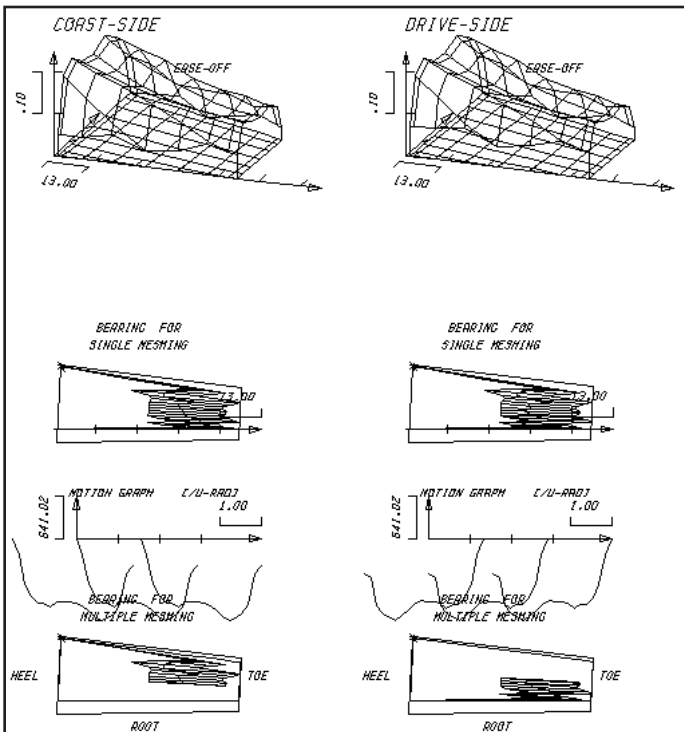

Figure 5   Ease-Off and TCA of high-traction design.

profile is a "textbook-like" duplication of the desired effect. The first derivative of the motion graph is the ratio modification (a fourth-order becomes a third-order).

It is remarkable that the tooth contact pattern still exists and a rolling without hard contact or interference lines occurs. The fuzzy left and right borders of the tooth contact can be explained by the dramatic Ease-Off and the numeric difficulties of the program algorithms to handle this complex tooth profile. However, it is expected that real machined high-traction differentials show some of this fuzzy appearance before the surfaces are broken in.

Practical results. The photograph (Fig. 6) shows a 7×12-tooth high-traction differential development, which is the subject of the discussions in this section. The teeth are coarse with respect to the size of the gears with a large whole depth of the teeth. This is required in order to provide sufficient profile depth for the functionality of the high-traction involute modulation.

Figure 7 shows on top the calculated motion transmission result of a 7×12-tooth differential (2 Nm gear torque simulated). The graphic underneath shows the motion graph as it was mea-
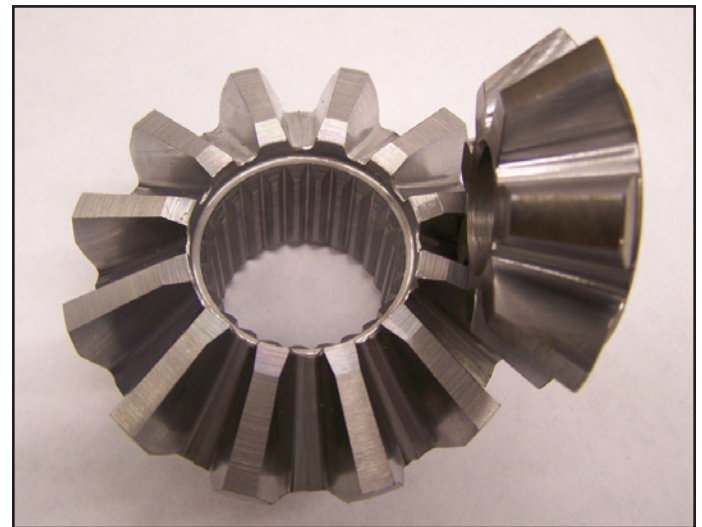

Figure 6   Practical example of a high-traction differential gear set.

sured on a single flank tester under 60rpm pinion speed and a gear torque of also 2 Nm. Between the intersecting points of the calculated motion (top) and the lower peaks of the graph, the displacement is 6,160 µrad. The lower graphic shows a displacement of only 4,000 µrad and the center peak of the calculated graph is smoothed out. The characteristic of both graphs, calculated and real measurement are very similar. This differential was manufactured applying the third-order function discussed in section "Solution."

The ratio change has been calculated by deriving the transmission graph according to gear roll angle. The result is shown in the two diagrams (Fig. 8, top). The first diagram is calculated

considering load-affected surface deflections for a gear torque of 50 Nm. The diagram underneath was calculated for a very low gear torque of 2 Nm. Low load seemed to cause more numerical instability of the calculations and lead to peaks. Random appearing peaks are caused by applying a derivative to a function which already contains waves and peaks. However, the red, S-shaped curve, or the straight line might reasonably represent the ideal form of the graph. The positive and negative amplitudes multiplied with the scaling factor of 0.02 result in a 7.6% ratio change along one tooth mesh. The desired ratio, due to 2 gear meshes, will be $1.076^2 = 1.15$, equal 15%.

The bottom graphic (Fig. 8) shows the angular velocity change. This numerical derivation was conducted from the measured single-flank data. The waviness of the climbing graph stems from the derivation of an already slightly wavy single-flank curve. Also here an S-shaped curve and a straight line were used to imply a realistic approximation of the graph. The magnitude of change is $\Delta W = 235{,}000$ μrad/sec i.e. —0.235 rad/sec. The angular velocity of the gear during the measurement was pinion $2\pi \cdot$ rpm/(ratio$\cdot$60) = 3.665 [rad/sec].

The maximal ratio change is calculated as:

$\Delta\omega/\omega = 0.235/3.665 = 0.064$, which is equivalent with 6.4% ratio change

The transmission of torque from the spinning wheel to the wheel with traction involves 2 tooth meshes — from the second-side gear to the pinion to the first-side gear. As such, the total ratio change is the square of the ratio factor (1.064):

Total ratio change = $1.064^2 = 1.13$, which is equivalent to 13% total ratio change.

High-traction kinematics. The case of traction on one wheel, represented by the locked lower side gear (Fig. 9) will cause a rotation of twice the speed of the upper-side gear, which slips in the present example. The pinion has to be shifted horizontally in order to generate realistic motions in the model. The lower tooth mesh moves the contact on the lower side gear tooth from root to top (gear drives pinion). This is equal to a reverse execution of the velocity change in the bottom graph (Fig. 8); in other words, it is attempted to reduce the velocity of the side gear. Since this is not possible, the pinion velocity in turn will be increased (acceleration). In the case of the upper mesh in Figure 9, the pinion drives the gear, where the tooth contact of the upper-side gear moves from top to root. This is consistent with an execution of the velocity graph at the bottom of Figure 8, from left to right.

Subsequently, this causes a speed increase of the upper side gear (acceleration). The addition of the accelerations caused
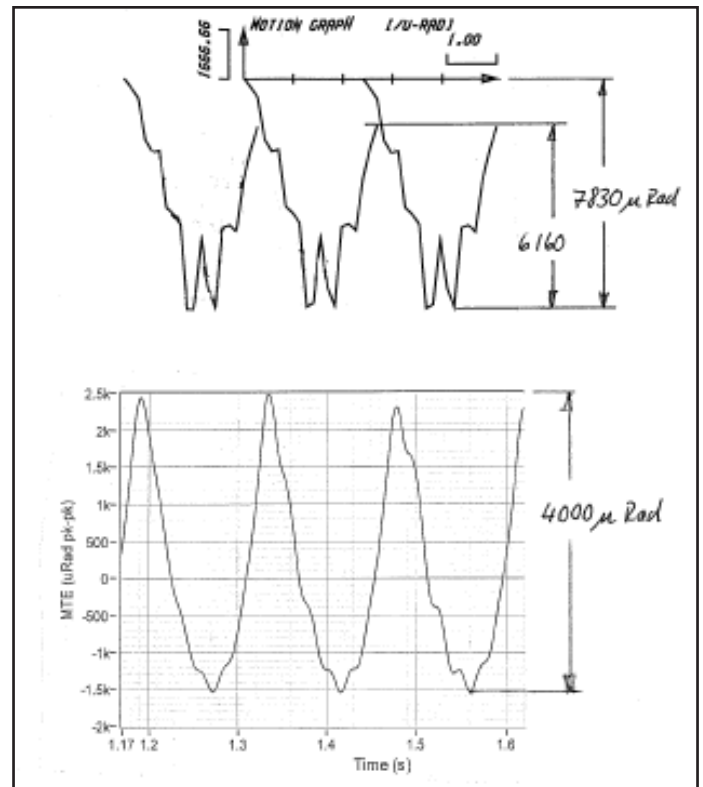

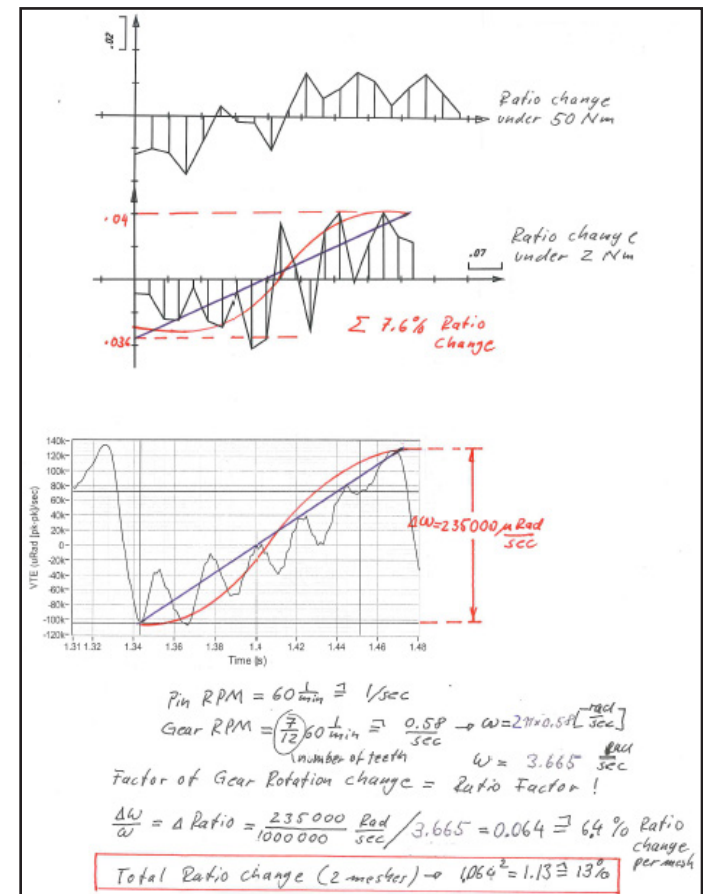**Figure 7 Motion graph, calculated (top) and real single-flank test (bottom).**

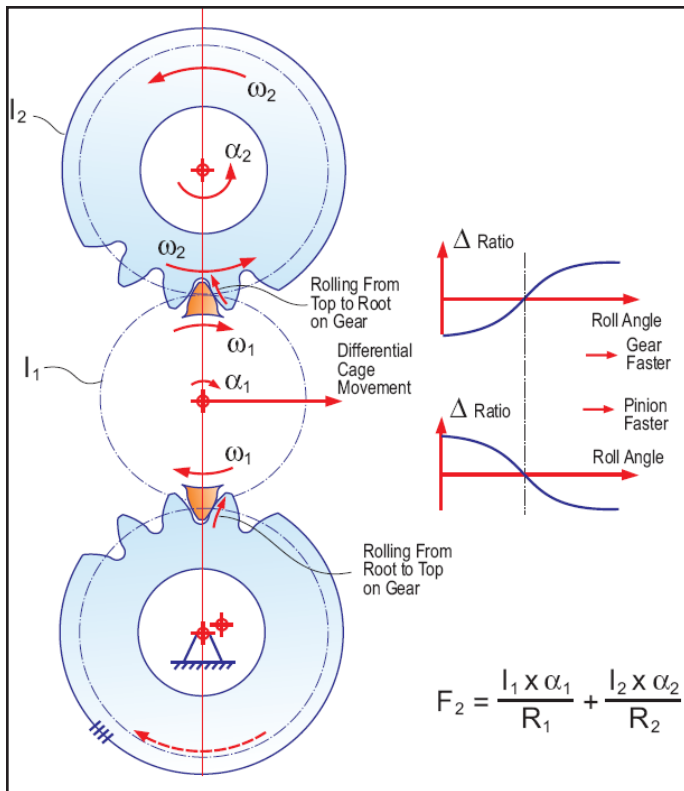**Figure 8 Calculated ratio change (top) and measured angular velocity variation (bottom).**

Figure 9   High-traction function, part 1.

$$F_2 = \frac{I_1 \times \alpha_1}{R_1} + \frac{I_2 \times \alpha_2}{R_2}$$

from the lower and upper tooth mesh multiplied with the inertia of the free spinning drive shaft and wheel creates a reaction force F_1. This reaction force F_1 plus a small force (from accelerating the differential pinion) will be generated in order to establish equilibrium in the differential unit. This reaction force F_2 (Fig. 10) at the bottom only lasts a fraction of one second. It is an active torque impulse, which is applied to the wheel with traction and causes a small vehicle movement.

As the unit keeps rotating and reaches the highest speed increase, the speed graph drops down and the speed increase repeats. The drop down will not cause a deceleration (negative force), but only eliminate the force for some milliseconds.

Final Remarks

High relative motion occurs in a differential only if one wheel spins free. Driving through curves only causes moderate relative motions. In case of high relative motion (like rolling the gearset on a roll tester) the high-traction differential causes certain vibration. Such a situation only happens in cases of traction loss of one wheel. Only then are the impulses in the tooth mesh detectable and lead to increased noise emission.

The high-traction differentials manufactured in the past had been machined on two tool generators. The third-order, modified ratio of roll that was applied as a roll cam modification might have arrived at the flank surfaces. However, in older machines with the typical generating flats, it is questionable if the 2 inflection points and the horizontal tangent at the pitch line of the high-traction modulation really arrived at the flank surfaces. So, when high-traction differentials were tested in the past and showed noisy and rough rolling on the roll tester, this was the only proof of a successful high-traction development. What
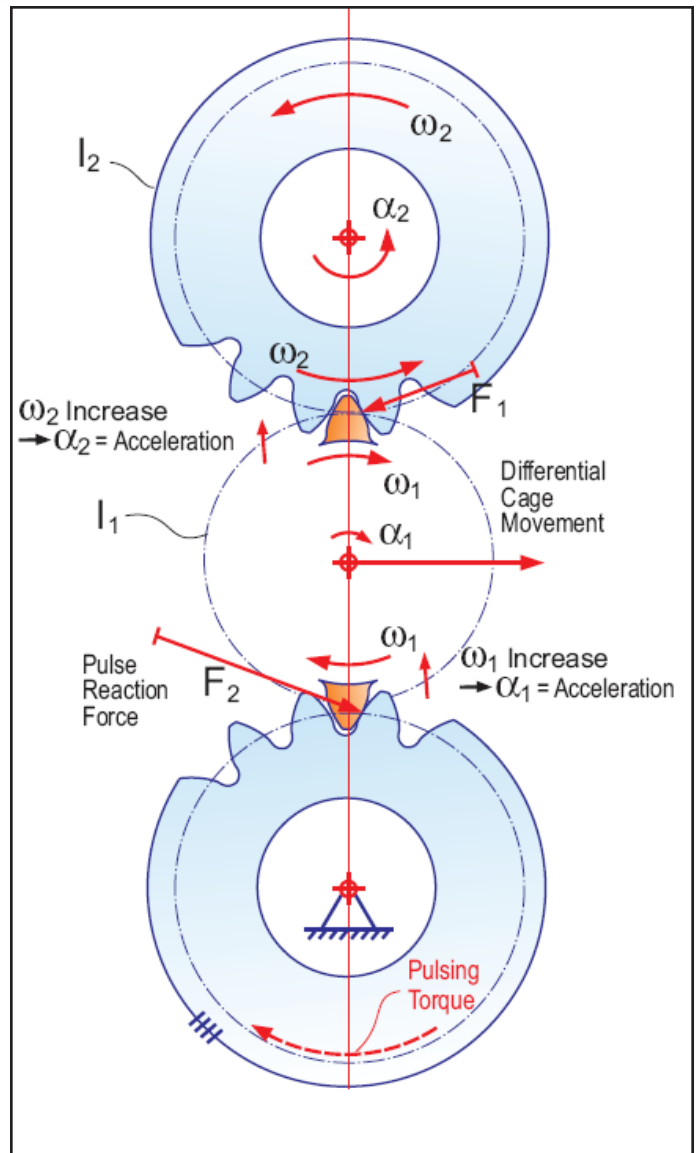

Figure 10   High-traction function, part 2.

a proof, considering the fact that a straight bevel gear set with a pressure angle error in one member also rumbles in the roll tester. There was no precise method of manufacturing high-traction differentials and no way to perform surface measurement against a theoretical master. In other words, the high-traction differentials of the past were "watered down" versions of what the inventors originally intended. Many of the high-traction differential gears have been converted to forging, where the die masters had been machined with 30-year-old two-tool generators. This was diminishing something that was already diminished and not much of the originally intended function was left.

The new method shown in this report allows to utilize a dry, high-speed carbide cutting process (PowerCutting) on modern CNC Phoenix free-form machines. The process is called ConiflexPlus and utilizes peripheral carbide stick blade cutters with Pentac blades. The curved root line versus the two-tool geometry can be minimized if a 15" cutter diameter is chosen. Surface finish and accuracy are high and AGMA quality 11 is standard. The manufactured gears can be measured against nominal flank surfaces, predetermined by the Coniflex analysis

software. Also, correction and a closed loop environment is a standard feature available for the new generation of high-traction differential gears. Today high-traction gears show their full potential. Compared to their predecessors, made on mechanical machines or forged, the new high-traction differential runs much smoother, with little noise, and their traction enhancement is excellent. ⚙
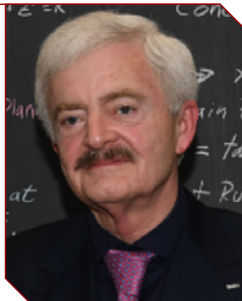
References
1. N.N.High-traction differential — a differential that "uses its head" Rockwell-Standard, 1969.
2. Pastor, A.Engineering Report No. 5181. Cam Calculation, Gleason, February 7, 2011, originated 1975 to 1977

For more information.
Questions or comments regarding this paper? Contact Dr. Stadtfeld at *hstadtfeld@gleason.com*.

Dr. Hermann J. Stadtfeld is the Vice President of Bevel Gear Technology and R&D at the Gleason Corporation and Professor of the Technical University of Ilmenau, Germany. As one of the world's most respected experts in bevel gear technology, he has published more than 300 technical papers and 10 books in this field. Likewise, he has filed international patent applications for more than 60 inventions based upon new gearing systems and gear manufacturing methods, as well as cutting tools and gear manufacturing machines. Under his leadership the world of bevel gear cutting has converted to environmentally friendly, dry machining of gears with significantly increased power density due to non-linear machine motions and new processes. Those developments also lower noise emission level and reduce energy consumption.

For 35 years, Dr. Stadtfeld has had a remarkable career within the field of bevel gear technology. Having received his Ph.D. with summa cum laude in 1987 at the Technical University in Aachen, Germany, he became the Head of Development & Engineering at Oerlikon-Bührle in Switzerland. He held a professor position at the Rochester Institute of Technology in Rochester, New York From 1992 to 1994. In 2000 as Vice President R&D he received in the name of The Gleason Works two Automotive Pace Awards — one for his high-speed dry cutting development and one for the successful development and implementation of the Universal Motion Concept (UMC). The UMC brought the conventional bevel gear geometry and its physical properties to a new level. In 2015, the Rochester Intellectual property Law Association elected Dr. Stadtfeld the "Distinguished Inventor of the Year." Between 2015–2016 CNN featured him as "Tech Hero" on a Website dedicated to technical innovators for his accomplishments regarding environmentally friendly gear manufacturing and technical advancements in gear efficiency.

Stadtfeld continues, along with his senior management position at Gleason Corporation, to mentor and advise graduate level Gleason employees, and he supervises Gleason-sponsored Master Thesis programs as professor of the Technical University of Ilmenau — thus helping to shape and ensure the future of gear technology.

For Related Articles Search

differentials

at www.geartechnology.com